

SHORT THESIS FOR THE DEGREE OF DOCTOR OF PHILOSOPHY (PHD)

Protein phosphatases regulate the activity of nitric oxide synthase and
the barrier function of endothelial cells

by Róbert Károly Bátori

Supervisor: Prof. Ferenc Erdődi



UNIVERSITY OF DEBRECEN
DOCTORAL SCHOOL OF MOLECULAR MEDICINE

DEBRECEN, 2018

Protein phosphatases regulate the activity of nitric oxide synthase and the barrier function of endothelial cells

By Róbert Károly Bátori, Biology/Biotechnology MSc

Supervisor: Ferenc Erdódi, DSc

Doctoral School of Molecular Medicine, University of Debrecen

Head of the **Examination Committee:** László Csernoch, PhD, DSc

Members of the Examination Committee: Attila Tóth, MD, PhD, DSc
Szabolcs Sipeki, PhD

The Examination takes place at the library of Faculty of Physiology, Faculty of Medicine, University of Debrecen at 9:30 am, 16th of December 2015.

Head of the **Defense Committee:** János Szöllősi, PhD, DSc, member of HAS

Reviewers: József Balla, MD, PhD, DSc
András Balla, PhD

Members of the Defense Committee: Attila Tóth, MD, PhD, DSc
Szabolcs Sipeki, PhD

The PhD Defense takes place at the Lecture Hall of Bldg. „A”, Department of Internal Medicine, Faculty of Medicine, University of Debrecen, at 13:00 pm, 4th of December 2018.

INTRODUCTION

The vascular endothelium

The vascular endothelium is composed of a single layer of closely connected endothelial cells (ECs) that lines the interior space of the blood vessels. One of the major functions of the endothelium is to provide a selective barrier between the blood and surrounding tissues, thus limiting the exit of cells, fluids, and high molecular weight substances from the blood vessels. This feature of ECs is termed semi-permeability. Maintenance of the semi-permeable endothelial barrier function requires a basal level of nitrogen-monoxide (NO), produced by endothelial nitric-oxide synthase (eNOS). The activity of eNOS, can be regulated by reversible phosphorylation/dephosphorylation. The endothelial barrier function is also dependent upon the activation of actomyosin contractile machinery, thus the phosphorylation level of myosin light chain 20 (MLC20) is an indicative of the endothelial barrier function. In response to inflammatory stimuli, the endothelial barrier can become compromised leading to severe, frequently fatal diseases. Thus, a better understanding of the mechanisms regulating the endothelial barrier function is imperative.

Regulation of the endothelial barrier function by reversible protein phosphorylation/dephosphorylation

The reversible protein phosphorylation catalyzed by protein kinases and protein phosphatases is one of the most common types of posttranslational modification. Protein phosphorylation is catalyzed by protein kinases that transfer the terminal γ -phosphate group of ATPs to serine (Ser), threonine (Thr) or tyrosine (Tyr) residues of proteins. Protein phosphatases ensure the reversibility of the process by hydrolyzing the phospho-ester linkage of the above residues. The human genome encodes 518 protein kinases that can be classified into Ser/Thr-, Tyr-, or dual specific protein kinases. The Ser/Thr specific kinases are responsible for 98.2% of all phosphorylation events within the cells. However, the number of protein phosphatases is less than one-third (only ~150 members) of the kinases of which less than 40 are P-Ser/Thr specific phosphatase catalytic subunit. Despite the smaller number of protein phosphatase catalytic subunits, diversity is achieved through their association with numerous regulatory subunits, forming holoenzymes with distinct activity and substrate specificity. According to the recent classification, phosphoprotein phosphatases (PPPs) can be classified into seven subclasses: protein

phosphatase 1 (PP1), -2A (PP2A) and -2B (PP2B, also termed calcineurin), and the novel protein phosphatases such as PP4, PP5, PP6, PP7. In the first part of our experiments we focused on the involvement of Ser/Thr-specific protein phosphatases in the regulation of eNOS and EC barrier function, therefore the characteristics of PP1 and PP2A will be summarized.

PP1

PP1 holoenzymes consist of a 35–38 kDa highly conserved catalytic subunit (PP1c), furthermore various regulatory subunits that provide substrate specificity. PP1c subunits in mammals are encoded by three genes and have five splice variants that are: PP1c α 1, PP1c α 2, PP1c γ 1, PP1c γ 2, and PP1c β (also termed as PP1c δ). The structure of PP1c shows compact folding with a central β -sandwich excluding the N- and C-terminals. The active site is located at the bifurcation center of a Y-shaped substrate binding groove. Although PP1c is catalytically active on its own, its substrate specificity is very low, which highlights the importance of the associated regulatory subunits. To date, PP1c has been reported to form functional complexes with over 200 targeting proteins that can regulate the catalytic activity of PP1c. A common feature of the regulatory subunits is that most of them interact with PP1 via a consensus sequence which is most commonly known as RVxF motif. Based on their function, the regulatory proteins can be classified into three distinct groups, which includes the inhibitors, substrate-specifiers (targeting subunits) and substrates. Among the targeting subunits, the MYPT-family has been well characterized in smooth muscle cells, but regulatory roles in non-muscle cells are also emerging.

PP2A

The heterotrimeric PP2A holoenzyme is comprised of a 36 kDa catalytic subunit (C), a 65 kDa scaffolding subunit (A), and a variable regulatory B subunit, but heterodimers (<10%) also exist. The A and C each have two isoforms (α and β), which are always associated, and together they form the heterodimer core enzyme (AC). The more dissociable regulatory B subunits can be classified into 4 structurally unrelated groups each encoded by 3-5 related genes. The B subunit family include the B, B', B'' and B'''. In contrast to PP1, the PP2A binding motifs on PP2A subunits or substrates have not yet been identified. The subunit combinations have an important role in modulating the substrate specificity and the catalytic activity of PP2A, which can also be regulated by posttranslational modifications. For instance, phosphorylation of the B' δ subunit on Ser566 by protein kinase-A can increase PP2A activity.

Regulation of PP1 and PP2A activity by phosphatase inhibitor toxins

Most of the protein phosphatases inhibitor toxins are membrane permeable non-selective phosphatase inhibitors. Both PP1c and PP2Ac activity can be inhibited by okadaic acid (OA), fostriecin, cantharidin and nodularin, microcystin-LR (MC-LR), calyculin-A (CLA) and tautomycin (TM), in a concentration-dependent manner. CLA and TM inhibit both PP1 and PP2A *in vitro*, however, their inhibitory effects in cellular systems remain controversial. In our experiments we have used CLA at a concentration (10 nM) that results in partial, but selective inhibition of PP2A, and TM (1 μ M) that results in predominant inhibition of PP1c.

Structure, regulation and function of myosin phosphatase

Myosin phosphatase holoenzyme (MP) was first isolated from chicken gizzard as a trimeric holoenzyme consisting of a ~38 kDa PP1c δ catalytic subunit, a 110-130 kDa myosin phosphatase targeting subunit 1 (MYPT1) and a small 20-21 kDa subunit (M20). The PP1c binding KVKF motif is located at the N-terminal region of MYPT1 isoforms between amino acids 35-38 flanked by an N-terminal arm that precedes the KVKF motif (amino acids 1-34), and the ankyrin repeat domains (8 repeats from amino acids 39-296). The main properties of MP can be attributed to a complex of PP1c δ and MYPT1 without M20 as a functional subunit. MYPT1 is important in determining the substrate specificity of MP via targeting the PP1 catalytic subunit to the diphospho-myosin light chain (ppMLC20). However, the multiple subcellular targets of MYPT1 suggests a much broader role of MP in cellular processes than only dephosphorylation of ppMLC20.

The regulation of MP in smooth muscle and in endothelial cells is similar. The activity of MP can be regulated by several ways. Among them the reversible phosphorylation of MYPT1 via Ser/Thr kinases, and the binding of inhibitory proteins have been intensively investigated. Two major inhibitory phosphorylation sites of MYPT1 are the Thr⁶⁹⁶ and Thr⁸⁵³ residues, which have a prominent role in the regulation of cell contractility. Both can be phosphorylated by ROCK leading to inhibition of MP. On the other hand, phosphorylation of MYPT1 at the adjacent serine residues, namely at Ser⁶⁹⁵ and Ser⁸⁵² in a cyclic nucleotide dependent manner by PKA/PKG prevents the inhibitory phosphorylation of MYPT1 at the Thr⁶⁹⁶ and Thr⁸⁵³ residues. However, dual-phosphorylation of these sites by PKA/PKG, at Ser⁶⁹⁵/Thr⁶⁹⁶ and/or Ser⁸⁵²/ Thr⁸⁵³ has also been reported with no significant effect on MP activity. Phosphorylation of Thr⁶⁹⁶ and Thr⁸⁵³ by ROCK

precludes the phosphorylation of the preceding Ser residues, thus phosphorylation of the Thr residues by PKA/PKG can only be observed when the preceding Ser residues are already phosphorylated. MP holoenzyme activity can also be regulated by interacting proteins. The most important endogenous inhibitor of MP holoenzyme is the small (17 kDa) protein phosphatase 1 regulatory subunit 14A also known as CPI-17. Unlike inhibitor-1 and inhibitor-2, CPI-17 inhibits both the PP1c δ catalytic subunit and the MP holoenzyme in a phosphorylation-dependent manner.

In ECs the reversible phosphorylation of MLC20 at Ser¹⁹ and subsequently at Thr¹⁸ by the Ca²⁺/calmodulin dependent MLCK and dephosphorylation by MP is essential for actomyosin contraction, which is a key step in the regulation of endothelial barrier function. Proinflammatory autacoids (e.g., histamine, bradykinin) induce MLCK activation in EC resulting in MLC20 phosphorylation and EC hyperpermeability. In contrast, extracellular purines e.g., adenosine (Ado), adenosine-triphosphate (ATP), and ATP γ S (a very slowly hydrolysable ATP analog) have been shown to be barrier protective in macrovascular ECs. Activation of PKA/PKG pathways by these agonists induces the phosphorylation of MYPT1 at Ser⁶⁹⁵ and Ser⁸⁵² preventing the phosphorylation and inactivation of MP by ROCK, thus leading to MLC20 dephosphorylation and cellular relaxation. It has been reported that a green tea polyphenol (-)-epigallocatechin-3-O-gallate (EGCG) activates PP2A in melanoma cells via cAMP/PKA dependent manner that results in dephosphorylation of MYPT1 at Thr⁶⁹⁶ and activation of MP.

Structure, regulation and function of eNOS

Nitric oxide (NO), is a highly diffusible and reactive free radical with a short half-life in biological fluids (~ 5 seconds). NO is synthesized by a family of enzymes collectively referred to as NO synthases (NOS). These are 3 isoforms of NOS, the neuronal- (nNOS), inducible- (iNOS), and the endothelial- (eNOS) nitric oxide synthase. eNOS is a constitutively expressed enzyme that is predominant in endothelial cells. The human eNOS is a 133 kDa multi-domain enzyme comprised of an N-terminal oxygenase, and a C-terminal reductase domain. Dimerization of eNOS monomers in head to tail orientation is required for NO production.

The primary mode of eNOS enzyme activation is through the elevated Ca²⁺ level which is required for Ca²⁺/CaM binding to each monomer. However, the activity of eNOS enzymes is meticulously controlled and involves multiple mechanisms at the transcriptional (e.g. via NF κ B, KLF-2, HIF1, and HIF2), posttranscriptional (TNF α) and posttranslational levels. At

posttranslational level, multiple kinases and phosphatases have been implicated in the regulation of eNOS activity through the phosphorylation of Ser, Thr and Tyr residues. Seven major phosphorylation sites have been described in human eNOS, but Ser1177 and Thr495 have special importance in regulation of eNOS activity. Both sites can be phosphorylated by multiple kinases. For instance phosphorylation of Ser1177 on a PKA dependent manner increases eNOS activity. In contrast, the phosphorylation of eNOS at Thr495 by Rho kinase or protein kinase C (PKC) negatively regulates the activity of eNOS. It also has been reported that stimulation of ECs with the PKC activator PMA, increases eNOS phosphorylation at Thr495 and reduces NO production.

Endothelial NOS and eNOS-derived NO are important regulators of numerous cardiovascular functions. In blood vessels, one of the most important biological actions of NO is the activation of the soluble guanylyl cyclase (sGC) and the subsequent generation of cGMP. The primary downstream target of cGMP in vascular smooth muscle is protein kinase G (PKG), which in turn activates MP, and promotes vasorelaxation. NO has multiple actions on endothelial barrier function as well. It has been demonstrated that inflammatory agonists that promote hyperpermeability such as VEGF increase NO levels which contribute to the leakiness of the endothelial barrier. However, pharmacological inhibition of NO synthesis or genetic deletion of eNOS also promotes the transendothelial leakage at the level of arterioles, capillaries, and postcapillary venules. In other studies, EGCG has been shown to elicits barrier protective effects on cultured endothelial cells, but the exact molecular mechanisms are not yet well understood.

AIMS

The molecular mechanisms regulating endothelial function have been intensively investigated over the past several decades and despite significant advances in our knowledge, the mechanisms involved in the preservation of endothelial barrier integrity are not yet fully understood. As discussed in the literature review, endothelium-derived NO plays a vital role in the regulation of numerous functions of blood vessels which includes changes in endothelial permeability. Dysregulation of eNOS phosphorylation and reduced expression of eNOS decreases NO bioavailability and is associated with increased severity of cardiovascular disease. Therefore, a better understanding of eNOS regulation and new approaches to improve eNOS function are important goals. The phosphorylation of eNOS at Thr495 has been shown to negatively influence the activity of eNOS and enzyme fidelity. Several kinases have been identified that mediate Thr495 phosphorylation, but the phosphatase holoenzyme with specific regulatory subunits and the signaling mechanisms mediating eNOS Thr495 dephosphorylation have not been described. ROCK phosphorylates eNOS at Thr495 and the amino acid sequences flanking this site show similarity to the phosphorylation sites of other ROCK substrates, which are often dephosphorylated by myosin phosphatase (MP), suggesting a possible involvement of this phosphatase in eNOS^{pT495} dephosphorylation. Thus, based on our preliminary data and the published literature my first aim was:

1. To investigate whether the MP holoenzyme is involved in the dephosphorylation of eNOS at Thr495 and to determine the underlying interactions and signaling mechanisms involved in eNOS inhibition or activation as well as in influencing the barrier function of endothelial cells.

On the other hand, Ado and ATP γ S are also important regulators of endothelial homeostasis that strengthen barrier function via cAMP-dependent and independent mechanisms, resulting in increased MP activity and consequently decreased MLC20 phosphorylation. The effect of Ado and ATP γ S on microvascular endothelial function remains poorly understood. Thus, my second aim was:

2. To define and compare the molecular mechanisms linking Ado- and ATP γ S-induced purinergic receptor activation and barrier strengthening processes in human lung microvascular endothelial cells (HLMVECs).

MATERIALS AND METHODS

Cell cultures

Human umbilical vein endothelial cells (HUVEC) were cultured in M199 media supplemented with 20% (v/v) fetal bovine serum (FBS), 10 mM HEPES, 2 mM L-glutamine, 0.25 µg/ml amphotericin B, 100 U/ml penicillin, 100 µg/ml streptomycin. Cells were cultured from the same batch and used at passages 4–7 for all experiments. Bovine pulmonary artery endothelial cells (BPAEC) were used between passages 17–23. Cells were cultured in MEM media supplemented with 10% (v/v) heat inactivated FBS, 1 mM sodium pyruvate, 0.1 mM non-essential amino acids solution, 2 mM glutamine, 1% (v/v) antibiotic-antimycotic solution. Human lung microvascular endothelial cells (HLMVECs) and human pulmonary artery endothelial cells (HPAEC) were cultured in EBM-2 and supplemented with 5-10% (v/v) FBS, 0.2 ml of hydrocortisone, 2 ml of human FGF-B, 0.5 ml of VEGF, 0.5 ml of R3-IGF-1, 0.5 ml of ascorbic acid, 0.5 ml of EGF, 0.5 ml of GA-1000, and 0.5 ml of heparin solutions. Human Embryonic Kidney cell line (HEK293), eNOS knock-in HEK293 and tsA201 cells were cultured in DMEM supplemented with 10% (v/v) FBS, 2 mM L-glutamine, and 1% (v/v) antibiotic-antimycotic solution. Cells were maintained at 37 °C, 5% CO₂ in a humidified atmosphere.

Immunoblotting

Protein samples were separated by SDS-PAGE and transferred to a 0.45 µM pore size nitrocellulose-, or 0.2 µM PVDF membrane at 100V for 1.5 h. The membranes were blocked with 5% (w/v) non-fat dry milk and 0.1% (v/v) Tween 20 containing solution in phosphate buffered saline PBST, alternatively in TBST when phospho-specific antibodies were used. The membranes were incubated for 3 hours at room temperature, or overnight at 4 °C with specific antibodies, then washed with PBST or TBST and incubated with horseradish-peroxidase (HRP) conjugated secondary antibodies. Immunoreactive proteins were developed with enhanced chemiluminescence (ECL) based method. The signals were detected either with FluorChem AIC system or on autoradiography films. Representative images were cropped from the whole blot images by Adobe Photoshop CS5 software. For densitometric analysis ImageJ software was used.

Transfection and gene silencing protocols

MYPT1 and/or eNOS was overexpressed in tsA201 cells at 70–80% confluency with DNA/PEI complex. In 100-100 μ l serum free medium, maximum 3 μ g DNA (2 μ g pcDNA3.1c-myc-eNOS plasmid alone, 1 μ g pM11-FLAG-MYPT1 alone or both expression vectors together) and 12 μ l jetPEI was pre-mixed and the diluted transfection reagent was added to the DNA. The mixture was incubated at room temperature for 30 min and added to the cells on 6 well plates, and the cells were incubated for 48 h before further analysis. HEK293 cells were transfected in 10 cm cell culture dishes with AKAP2 and MYPT1 coding expression vectors using X-tremeGENE™ HP DNA transfection reagent. In 600 μ l serum free medium first 6 μ g DNA, then 18 μ l X-tremeGENE™ HP DNA transfection reagent was added and incubated for 25 minutes at room temperature. The transfection mixture was added to the cells in complete media containing 10% FBS and incubated for 48 hours at 37 °C.

For gene silencing experiments BPAE or HLMVEC cells were seeded on 6 well plates and transfected with non-specific (scrambled), pan PP1c, MYPT1, EPAC1, AKAP2, PKA α or P2Y receptor specific siRNA in 20-50 nM final concentration using DharmaFect 2 or siPORT™ Amine transfection reagents, according to the manufacturers instructions. After 6 hours of incubation FBS was supplemented to the cell cultures in 20% final concentration, followed by 48 h further incubation, or the media was changed to complete EBM-2 and the cells were incubated for 72 hours at 37 °C.

Nitric-oxide measurement

NO-content of the cell culture medium was determined by Sievers NO Analyzer NOA 280i according to the manufacturer's instructions. After 30 minutes or 48 hours of incubation the NO formed in the cells diffused to the medium and was converted to nitrite in the presence of oxygen. The protein content of cell culture medium was precipitated with 200 mM ZnSO₄. One hundred microliters of each sample were applied to the reaction chamber, where nitrite was converted to NO by sodium iodide and was liberated by purging. The NO liberated was converted by ozone to electrically excited nitrogen-dioxide (NO₂*). The emission from NO₂* is in the near-infrared spectra which is detected by a photomultiplier tube. The light emitted is equivalent with the NO formed in the cells.

Nitric-oxide measurement with DAF-2 DA

The BPAE were seeded on 13 mm diameter coverslips in 24 well plates. The cells were cultured until 60-80 % of confluence. The culturing media was then replaced with the reaction buffer, consisting of 1 μ M β -NADH, arginine substrate, 25 μ M 4,5-diaminofluorescein diacetate (DAF-2 DA) and the cells were incubated for 2 hours at 37 °C. Then PMA or EGCG was added to the corresponding wells for 1 hour. In parallel, non-treated coverslips (control) were also incubated with reaction buffer. The cells were washed with PBS and fixed in 4% (v/v) paraformaldehyde (PFA) solution for 10 minutes at room temperature. After washing three times with PBS, the samples were mounted with 4.3 (m/v) Mowiol and prepared for confocal microscopy.

Pull-down assays

GST-MYPT1 pull-down experiments were carried out by coupling of GST (in control experiments) or GST-MYPT1 to glutathione-Sepharose beads, then the HUVEC lysate was applied to the resin and incubated for 3 hours at 4 °C. The resin was washed three times with washing buffer, then boiled for 10 minutes with SDS sample buffer and subjected to immunoblot analysis with the anti-eNOS antibody. Pull-down of overexpressed c-myc-eNOS or FLAG-MYPT1 from tsA201 cell lysate were carried out using anti-c-myc and anti-FLAG M2 antibody-coupled EZview™ Red affinity gel and analysed with anti-MYPT1 and anti-eNOS or with anti-c-myc and anti-FLAG antibodies.

***In vitro* phosphorylation/dephosphorylation assays**

C-myc-eNOS was overexpressed in tsA201 cells and the cells were lysed in lysis buffer, centrifuged (10 000 g, 10 min) and the supernatant was bound to EZview™ Red anti-c-myc affinity gel. After the binding process the gel was washed three times, and the affinity gel matrix was resuspended in ROCK assay buffer at the presence of 1 μ M MC-LR. Twenty percent of the gel was removed and boiled in hot SDS sample buffer. Phosphorylation of c-myc-eNOS was started by addition of 0.2 mM ATP in the presence of 5 mU/mL ROCK, and the mixture was incubated for 1 hour, followed by 6 washing steps with 20 mM Tris-HCl (pH 7.5) buffer to remove MC-LR, ATP, and Mg²⁺. The gel was resuspended again in 100 μ l 20 mM Tris-HCl (pH 7.5) buffer and another 20% of the initial gel amount was removed and boiled in SDS sample buffer. The ROCK-phosphorylated sample was divided into three equal aliquots and was incubated for 15 min with 15 nM purified FLAG-MYPT1, 5 nM purified native rabbit skeletal muscle PP1c or 5 nM PP1c

plus 15 nM FLAG-MYPT1. The reactions were stopped with hot SDS sample buffer, then the samples were boiled for 5 minutes and subjected to immunoblotting.

Assay of protein phosphatase activity

Prior to treatments, BPAECs were incubated in serum-free medium for 16 h, then the cells were treated with 10 nM CLA for 30 min, 20 μ M EGCG for 1 hour. Cells were centrifuged at 600 g for 5 min, and washed with PBS followed by washing with TBS containing 0.1 mM EDTA. Cells were resuspended in 100 μ l ice-cold TBS containing 0.1 mM EDTA supplemented with 0.5% (v/v) protease inhibitor cocktail and 50 mM 2-mercaptoethanol. Cells were lysed by sonication on ice, then clarified by centrifugation (13000 g, 10 min). The phosphatase activity of the supernatants was determined at 30 °C in 20 mM Tris-HCl (pH 7.4) buffer with 1 μ M 32 P-MLC20 in the absence or presence of 2 μ M His-inhibitor-2 (I2). The reaction was initiated by addition of the substrate. After a 10 min, the reaction was terminated by the addition of 200 μ l 10% TCA and 200 μ l 6 mg/ml BSA. The precipitated proteins were collected by centrifugation, and the released 32 P_i was determined from the supernatant in a scintillation counter.

Immunofluorescence and confocal microscopy

BPAECs and HPAECs were plated on gelatin-coated glass coverslips and were grown for 24 hours. After fixation with 4% (v/v) PFA for 10 minutes, the cells were permeabilized with 0.1% Triton X-100 containing buffer for 1 hour followed by three washing steps with 4% (w/v) BSA in PBS and once with antibody diluting solution. After blocking the cells were incubated overnight at 4 °C with anti-eNOS, or with anti-MYPT1¹⁻²⁹⁶ antibodies. Next, the cells were washed three times with PBS and incubated with Alexa-488 or Alexa-546 labeled secondary antibodies for 1 hour at room temperature. Finally, the cells were covered in Prolong Gold Antifade mounting medium. The localization of eNOS and MYPT1 was visualized using a confocal microscope. The optical thickness of the co-localization images was 1 μ m.

Duolink proximity ligation assay

BPAECs cultured in 24 well plates on glass coverslips were fixed after treatment with 4% PFA solution for 10 minutes, permeabilized with 0.1% Triton X-100 for 10 minutes and blocked with 5% BSA in PBS. The proximity ligation assay (PLA) was carried out according to the manufacturer's instructions. Briefly, to visualize the interaction between eNOS and MYPT1 the

samples were stained with mouse anti-eNOS and rabbit anti-MYPT1¹⁻²⁹⁶ antibodies overnight, at 4 °C prior to incubation with PLA probes for 1 hour at 37 °C. Then, ligase was added to connect the probes and after the rolling-circle amplification (RCA) the labeled probes were hybridized to the RCA product. After washing three times with PBS, the samples were mounted with 4.3 % (m/v) Mowiol and prepared for confocal microscopy.

Surface plasmon resonance measurement

Interaction of GST-MYPT1 with c-myc-eNOS was analyzed by surface plasmon resonance-based binding experiments using a Biacore 3000 instrument. Anti-GST was immobilized on CM5 sensor chip by amine-coupling according to the instructions of the manufacturers. On one surface recombinant GST while on the two other surfaces full-length GST-MYPT1 were immobilized in running buffer. C-myc-eNOS at 0.5 μ M or 1 μ M in running buffer was injected over the surfaces, and the amount of the captured analyte was determined from the changes of the resonance signal. The surface (with immobilized recombinant GST) was treated identically to the GST-MYPT1 surfaces to determine unspecific binding which was subtracted from the data obtained with the GST-MYPT1 surfaces.

Transendothelial permeability measurement

Transendothelial electrical resistance (TER) of BPAECs and HLMVECs were measured using electric cell-substrate impedance sensing (ECIS) instrument, Model 1600R. Approximately equal numbers of BPAECs or HLMVECs were seeded on ECIS arrays (8W10E), and the experiments were performed when the resistance values of the wells achieved $\geq 1000 \Omega$ of baseline steady-state resistance. An hour prior treatment BPAECs media was changed to serum-free MEM and changes in the resistance values were monitored after treatments with PMA, CLA TM or EGCG. When HLMVECs were analyzed, six hours before treatment cell culture media was changed to complete EBM-2 and changes in the initial resistance were recorded when the basal resistance was stable. HLMVECs were treated with Ado or ATP γ S agonists, and the collected data were normalized to the initial resistance values and plotted as normalized resistance.

Quantitative real-time PCR (qPCR)

Total RNA was isolated using Trizol reagent according to the manufacturer's instructions. cDNA synthesis was conducted using iScript cDNA Synthesis Kit and 1 μ g RNA template. 7.5x diluted

cDNA was used for quantitative PCR (qPCR) reactions. qPCR was performed using a Qiagen Rotor-Gene Q system and iQ™ SYBR Green supermix. Data were analyzed using internal tools.

cAMP measurement

HLMVECs cultured in 6 well plates were treated at 90% confluency with 100 μ M Ado or ATP γ S for 30 minutes. After washing with 1 ml PBS, HLMVECs were incubated in 250 μ l, 0.1 M HCl at room temperature for 20 minutes, then scraped, and the mixture was further processed by pipetting up and down until the suspension became homogeneous. The cell lysate was centrifuged at 1000 g for 10 minutes, then cAMP was measured from the supernatant by using a cyclic AMP EIA kit according to the manufacturer's instructions.

PKA activity measurement

HLMVECs were incubated in the absence or presence of 50 μ M Ado or ATP γ S for 30 minutes, then the cells were washed three times with 1 ml ice cold PBS on ice and lysed in 20 mM MOPS, 50 mM β -glycerolphosphate, 50 mM sodium fluoride, 1 mM sodium orthovanadate, 5 mM EGTA, 2 mM EDTA, 1% NP-40, 1 mM AEBSF and 1% (v/v) protease inhibitor cocktail containing lysis buffer. PKA activities were measured using a commercial kit according to the manufacturer's instructions. Briefly, 96 well assay plates pre-coated with PKA specific substrate were incubated with the extracted proteins (1 μ g/well) in the presence of ATP and PKA activity was revealed with a phospho-specific substrate antibody.

RESULTS AND DISCUSSION

Identification of the interaction between the regulatory subunit of MP (MYPT1) and eNOS

To prove that eNOS is a possible substrate of MP, first we assessed if eNOS and MYPT1 interact in ECs. Thus, we performed pull-down experiments from HUVEC by GST-MYPT1 capturing recombinant GST-MYPT1 and the associated endothelial proteins on glutathione-Sepharose matrix. eNOS was identified in the eluate on immunoblots, suggesting its co-precipitation with GST-MYPT1, whereas no eNOS was detected in control GST-pull-down fraction. Immunoprecipitations from the lysates of tsA201 cells co-expressing both FLAG-MYPT1 and c-myc-eNOS proteins also were analyzed, and these data confirmed reciprocal co-immunoprecipitation of c-myc-eNOS and FLAG-MYPT1 with each other. To further demonstrate the interaction of MYPT1 and eNOS, purified c-myc-eNOS was applied as an analyte to surface plasmon resonance based binding assays to assess its interaction with GST-MYPT1 immobilized on the anti-GST coupled sensor chip. The sensorgrams indicated stable interaction of MYPT1 with eNOS that was reversible.

Interactions of eNOS and MYPT1 were visualized *in situ* in BPAEC and HPAEC at the perinuclear regions using confocal microscopy. This interaction was confirmed by proximity ligation assay as well. Thus, the above data suggest that eNOS and MYPT1 interact in ECs implying that MP may be a possible PP1 holoenzyme candidate involved in the dephosphorylation of eNOS.

The effects of eNOS phosphorylation level on NO production

TsA201 cells do not express eNOS, however, they are assumed to include the kinase/phosphatase machinery able to phosphorylate/dephosphorylate eNOS and MYPT1. Thus, tsA201 cells transfected with c-myc-eNOS construct appeared to be a suitable model system to assess phosphorylation/dephosphorylation of eNOS upon PKC activation and phosphatase inhibition by calyculin-A (CLA), a cell-permeable toxin inhibitor of PP1 and PP2A. We found that in c-myc-eNOS expressing cells there is a basal level of eNOS phosphorylation at Ser1177 (eNOS^{pSer1177}), while eNOS^{pThr495} is very low. In agreement with the low level of the inhibitory phosphorylation (eNOS^{pThr495}) and in the presence of activator phosphorylation (eNOS^{pSer1177}) eNOS expressing tsA201 cells produced a significant amount of NO. Activation of PKC by treatment of tsA201 cells with PMA alone, or in combination with CLA, increased the level of

eNOS^{pThr495} by ~4- or ~7-fold, respectively. On the other hand, the level of eNOS^{pSer1177} was slightly enhanced only. PMA or PMA plus CLA treatments dramatically suppressed the NO production of eNOS expressing tsA201 cells. These data confirm previous suggestions that phosphorylation of eNOS at Thr495 is a significant determinant in the regulation of eNOS activity.

The effects of MYPT1 and eNOS co-expression on NO production

To test whether MYPT1 overexpression may influence eNOS activity we overexpressed both, FLAG-MYPT1 and c-myc-eNOS in tsA201 cells. NO production was not induced when FLAG-MYPT1 was overexpressed alone. When c-myc-eNOS was overexpressed, NO synthesis was detected, which was significantly higher when FLAG-MYPT1 was co-expressed with c-myc-eNOS. These data implicate MYPT1 in the regulation of eNOS activity and NO production. To further confirm the above data, we also carried out experiments with HEK293-eNOS cells in which FLAG-MYPT1 was overexpressed. In accord with the previous experiments, the NO production in HEK293-eNOS cells was significantly higher compared to HEK293 cells, which do not express eNOS. The NOS inhibitor L-NAME treatment suppressed the increased eNOS activity to control level in both, non-transfected and FLAG-MYPT1 transfected HEK293-eNOS cells. Surprisingly neither the expression nor the phosphorylation level of eNOS^{pThr495} was changed under our experimental conditions. We speculate that the interaction between eNOS and MYPT1 might influence intracellular localization of eNOS, which can also affect the NO production.

MP dephosphorylates eNOS at Thr495 *in vitro*

It has been already shown that PP1 can dephosphorylate eNOS at Thr495, although, it is unclear whether MYPT1 can facilitate the dephosphorylation of eNOS at this phosphorylated residue. Thus, c-myc-eNOS was phosphorylated by ROCK at Thr495 on anti-c-myc-Sepharose beads and this phosphorylated eNOS was subjected to dephosphorylation via PP1c, FLAG-MYPT1, and PP1c plus FLAG-MYPT1. We show that FLAG-MYPT1 was without effect, while PP1c alone dephosphorylated eNOS^{pThr495} to a relatively low extent, which was significantly increased when both PP1c and FLAG-MYPT1 were present. These results suggest that MP holoenzyme (i.e. the PP1c-MYPT1 complex) is an eNOS^{pThr495} phosphatase. To further confirm the role of PP1c and MYPT1 in the dephosphorylation of eNOS^{pThr495} depletion experiments of were carried out in BPAECs and, the level of eNOS^{pThr495} was determined. PP1c was depleted with siRNA specific for all isoform (PP1 α , PP1 β/δ , PP1 γ 1), however, decrease in the level of PP1 δ

was assessed as this isoform was identified to associate with MYPT1 specifically in cells. Depletion of PP1 δ , MYPT1 or both, was accompanied by an increase in the level of eNOS^{pThr495} implicating both subunits of MP holoenzyme in the dephosphorylation of this phosphorylated residue.

The effects of phosphatase inhibitors on the inhibitory phosphorylation of MYPT1 and eNOS

We challenged BPAECs with 10 nM calyculin-A (CLA) or 1 μ M tautomycin (TM) to inhibit PP2A and PP1, respectively. Treatment of BPAECs with CLA alone resulted in a dramatic increase in the phosphorylation of MYPT1 at Thr696 (MYPT1^{pThr696}) while TM and PMA did not increase the level of MYPT1^{pThr696} significantly. Enhanced level of MYPT1^{pThr696} paralleled with the increase of the inhibitory phosphorylation of eNOS^{pThr495}. In contrast, TM slightly increased the level of eNOS^{pThr495}. Activation of PKC by PMA also increased the level of eNOS^{pThr495} in accordance with results shown for eNOS expressing tsA201 cells. As PP2A is assumed to dephosphorylate MYPT1^{pThr696}, the above data support the scenario that PP2A specific inhibition increased the level of MYPT1^{pThr696} resulting in inhibition of MP and suppression of eNOS activity consequently resulting in an increase of eNOS^{pThr495}.

To specifically inhibit PP1 and identify the type-specific inhibition by CLA, we determined the distribution of the activity of PP1 and PP2A in the lysates of untreated or CLA treated BPAECs using PP1-specific phosphatase inhibitor-2 (I2). It is seen that ~65% of the total phosphatase activity was due to PP1 while PP2A (the activity measured in the presence of I2) represented ~35%. CLA decreased the phosphatase activity of the lysate by ~25%, and a large portion (~20%) of this inhibitory impact was exerted on the I2 suppressed (i.e., PP2A) activity indicating predominant inhibition of PP2A by CLA in endothelial cells.

Investigation of eNOS^{pThr495} dephosphorylation upon EGCG induced PP2A mediated MP activation

Our data suggest a PP2A mediated MYPT1^{pThr696}, and as a result eNOS^{pThr495} dephosphorylation but this putative mechanism required further confirmation. Therefore, activation of PP2A in BPAECs and subsequent dephosphorylation of both MYPT1^{pThr696} and eNOS^{pThr495} were probed. It was previously shown that in melanoma cells EGCG binds to the 67 kDa laminin receptor (67LR) and increases PP2A activity in a PKA dependent manner. This activation of PP2A was shown earlier to be specific for the PP2A trimer holoenzyme including the B δ subunit and was due to phosphorylation of B δ by PKA. We confirmed that both PP2A-B δ and

67LR are present in BPAECs, therefore we attempted to activate PP2A with EGCG. EGCG treatment resulted in substantial decrease in the levels of both MYPT1^{pThr696} and eNOS^{pThr495}, suggesting that PP2A is involved in their dephosphorylation. Moreover, EGCG also significantly increased the phosphatase activity, and dephosphorylation of 20 kDa light chain of myosin II (MLC20) as assessed by an antibody specific for dual phosphorylated MLC20 at Thr18/Ser19 (ppMLC20).

To demonstrate the PKA dependence of EGCG induced dephosphorylation processes we silenced the catalytic subunit α of PKA (PKA α) in BPAECs and assessed the level of MYPT1^{pThr696}, eNOS^{pThr495} and ppMLC20. The transfection of BPAECs with scrambled siRNA resulted in similar patterns of MYPT1^{pThr696}, eNOS^{pThr495} and ppMLC20 dephosphorylation upon EGCG treatments as observed in the previous experiment. In BPAECs transfected with PKA α specific siRNAs a slight decrease in the basal phosphorylation of MYPT1^{pThr696}, eNOS^{pThr495} and ppMLC20 were observed, however, no significant dephosphorylation of these proteins were detected upon challenges by EGCG. These data confirmed that EGCG induced phosphatase activation in BPAECs is also accomplished in a PKA dependent manner.

The effects of PKC activation and phosphatase inhibition/activation on NO production and transendothelial electrical resistance (TER) of BPAECs

For NO measurement NO specific 4,5-diaminofluorescein diacetate (DAF-2 DA) fluorescence of cells was captured. PMA moderately, but significantly decreased NO synthesis. In contrast, EGCG spectacularly enhanced NO production, and it also attenuated PMA suppressed NO synthesis. These changes in NO synthesis correlate well with the influence of these effectors on the phosphorylation level of eNOS^{pThr495}.

PMA and TM suppressed TER moderately, and the decreasing tendency in TER appeared to be partially reversible in case of PMA, but irreversible with TM during the assay period. CLA also induced a fast and dramatic decrease in TER in an irreversible manner. This “acute” effect of the phosphatase inhibitors on TER was presumably due to the inhibition of MP resulting in sustained phosphorylation of MLC20 which highly contributes to decreasing TER. In contrast, EGCG enhanced TER of BPAECs and attenuated PMA induced suppression of TER either when it was added together or 30 min after PMA treatment. These data suggest that phosphatase

activation by EGCG improves barrier function and helps to restore, at least in part, the effect of barrier suppressing agents.

Investigation of the barrier function of HLMVECs upon Ado and ATP γ S administration

It has long been known that extracellular purines function as intercellular signaling molecules that may positively affect the barrier function of macrovascular endothelial cells, however, their effects on microvascular endothelium are less explored. Thus, we examined the effects of Ado and ATP γ S which is a very slowly hydrolysable ATP analog, on HLMVEC barrier function. First, we challenged HLMVECs with increasing concentrations (25-200 μ M) of Ado or ATP γ S and TER was measured. Both Ado and ATP γ S induced TER increase of HLMVECs in a dose-dependent manner, reflecting HLMVEC barrier strengthening with maximal effect at 100 μ M. As such, we used 50 or 100 μ M Ado or ATP γ S in subsequent experiments.

Mapping of the expression of purinergic receptors in HLMVECs

Extracellular Ado initiate its effects via cell surface P1-, while ATP γ S exert its effect by binding P2 purinergic receptors. The P1 Ado receptors are divided into four subclasses, namely A1, A2A, A2B and A3. The A1 and A3 receptors are coupled to G_i proteins that inhibit adenylyl cyclase, while A2A and A2B are G_s protein-coupled receptors, therefore can increase intracellular cyclic-AMP (cAMP) level. P2 receptors are divided into two subclasses: the P2X (P2X1-7) receptors are extracellular ATP-gated, calcium-permeable, non-selective cation channels, that are unlikely to be involved in the endothelial barrier regulation; while P2Y receptors (P2Y1, P2Y2, P2Y4, P2Y6, P2Y11-14) are G-protein coupled receptors. The expression pattern of purinergic receptors in ECs from different regions of the vasculature is variable and ambiguously described. We provided a comprehensive analysis of G-protein coupled P1 and P2Y receptor mRNA expression pattern in HLMVECs using qPCR. Our data showed that among P1 adenosine receptors HLMVECs expressed A2B receptors alone with a negligible expression of other adenosine receptor subtypes. This expression pattern significantly differs compared to HUVEC and also vary that as detected in HPAEC suggesting differences in P1 receptor signaling in ECs from different vascular beds. Analysis of P2Y receptors profile revealed that HLMVECs express mRNAs of all eight receptor types with preferential expression of P2Y1, 4, 6, 13 and 14 mRNAs, while the expression level of other receptor subtypes was lower.

Ado and ATP γ S increase PKA activity by different signaling mechanisms

It has been shown that PKA activation is a requirement for Ado- and ATP-induced barrier strengthening in HPAEC. The primary activation pathway for PKA involves the binding of four cAMP molecules to the regulatory subunit leading to dissociation of the holoenzyme. While the G_s-mediated cAMP-dependent activation of PKA by Ado is well described, cAMP-independent mechanisms of PKA activation are poorly understood.

Our data indicate that Ado treatment induced immediate elevation of cAMP levels in HLMVEC, culminating at 30-45 minutes which paralleled with Ado-induced TER increase. In contrast, ATP γ S-induced HLMVEC barrier enhancement accompanied by modest, but significant cAMP decrease, supporting the involvement of G_i-mediated signaling in ATP γ S-induced HLMVEC barrier enhancement. In a parallel experiment, we examined the effect of Ado and ATP γ S on PKA activity in HLMVEC homogenates. We found that both compounds induced significant activation of PKA after 30 min of treatment. This is accompanied by increased MYPT1 dual phosphorylation at Ser695/Thr696, which are established PKA phosphorylation sites. These data strongly suggest that ATP γ S activates PKA via an unconventional G_i-mediated pathway. Since PKA-mediated phosphorylation of MYPT1 is involved in the regulation of MP activity, at least *in vitro*, these data also suggest that the effects of PKA on ATP γ S-induced HLMVEC barrier enhancement are MP-dependent.

Investigation of the involvement of EPAC1 and PKA in Ado- and ATP γ S-induced HLMVEC barrier enhancement

To directly evaluate the role of PKA activity in HLMVEC barrier strengthening induced by either Ado or ATP γ S, we next examined the effects of PKAc depletion on the phosphorylation state of MLC20. In control, non-specific siRNA transfected cells both Ado and ATP γ S decreased the phosphorylation level of MLC20 at Thr18/Ser19 phosphorylation sites, as anticipated. However, depletion of PKAc abolished ATP γ S, but not Ado-induced MLC20 dephosphorylation, suggesting the involvement of another signaling pathway that is stimulated by Ado. Since EPAC1, the other cAMP effector has been reported to be involved in SM relaxation and regulation of MLC20 dephosphorylation, we investigated the involvement of EPAC1 in Ado-induced MLC20 dephosphorylation in HLMVEC. Predictably, EPAC1 depletion had no effect on cAMP-independent ATP γ S-induced MLC20 dephosphorylation, but surprisingly, had no effect on Ado-

induced cAMP-dependent MLC20 dephosphorylation either. Simultaneous depletion of PKAc and EPAC1 in double knock-down experiment abolished Ado-induced MLC20 dephosphorylation indicating that both PKA and EPAC1 activities are simultaneously required to achieve MLC20 dephosphorylation in cAMP-dependent Ado model.

To examine the role of PKA and EPAC1 in HLMVEC barrier strengthening, we depleted PKAc, and EPAC1, then challenged HLMVECs with Ado or ATP γ S and measured TER. We found that PKAc silencing significantly attenuated ATP γ S- but not Ado-induced effects on TER. However, depletion of EPAC1 had no effect on TER changes induced by either Ado or ATP γ S. In accord with the effects on MLC20 phosphorylation, simultaneous depletion of PKAc and EPAC1 attenuated Ado-induced TER increase indicating that PKA effects on EC barrier properties are EPAC1-dependent. Simultaneous depletion of PKAc and EPAC1 decreased ATP γ S-induced increase in TER to a similar extent as depletion of PKAc alone, indicating that EPAC1 is not involved in G $_i$ -mediated ATP γ S-induced EC barrier enhancement. These data suggest that while PKA alone is sufficient to exert a barrier-enhancing effect in ATP γ S model, Ado-induced EC barrier strengthening requires simultaneous activation of both PKA and EPAC1.

AKAP2-MP axis is involved in ATP γ S barrier-enhancing effect in HLMVEC

Scaffolding PKA-binding AKAP proteins exert their activities via directing PKA to specific subcellular targets also and serve as a platform for biochemical interactions. It has been shown that cAMP-independent PKA activation may involve AKAPs. Furthermore, specific AKAPs namely AKAP9 and -12 are involved in EC barrier regulation, although in a cAMP-dependent manner. Thus, we examined whether depletion of AKAPs influences the Ado- and ATP γ S-induced TER increases, and MLC20 phosphorylation. Our data indicate that neither depletion of AKAP9 nor AKAP12 attenuated ATP γ S or Ado-induced barrier enhancing effects in HLMVEC. However, depletion of another member of the AKAP family, namely AKAP2 attenuated the effect of ATP γ S, but not Ado on TER, suggesting a dominant role for AKAP2 in ATP γ S induced, cAMP-independent PKA activation.

To investigate the direct involvement of AKAP2 in ATP γ S-, and Ado-induced MLC20 dephosphorylation gene silencing experiments were performed. Our data show, that AKAP2 has a prominent role in ATP γ S-, but not in Ado-induced MLC20 dephosphorylation. Interaction of AKAPs and PP1-containing holoenzymes has been previously reported; however, the interaction

of AKAP(s) with MYPT1 has not been described. Therefore, we investigated whether AKAP2 or other AKAPs could interact with MYPT1. Our co-immunoprecipitation experiments demonstrate that MYPT1 can be co-immunoprecipitated with AKAP2 but not with AKAP3, AKAP9 or AKAP12, suggesting the existence of a specific functional complex between AKAP2 and MP. Reciprocal experiments further supported the interaction (direct or indirect) of AKAP2 and MYPT1. Moreover, our results provided evidence of PKAc and G_{i2} co-immunoprecipitation with AKAP2 in HLMVECs suggesting the scaffolding role of AKAP2 in G_i-mediated PKA activation.

SUMMARY

The importance of eNOS to cardiovascular homeostasis has been well established. A major regulator of the activity of eNOS is post-translational phosphorylation and in particular the inhibitory phosphorylation at Thr495. Through the use of various biochemical and molecular biological techniques we have demonstrated that the myosin phosphatase (MP) holoenzyme, comprised of protein phosphatase-1 catalytic subunit (PP1c) and the MP target subunit-1 (MYPT1), is a bona fide eNOS^{pThr495} phosphatase. MYPT1 plays a regulatory role by guiding PP1c toward the eNOS^{pThr495} substrate. Inhibitory phosphorylation of MYPT1 at Thr696 can thus impact the action of MP on eNOS^{pThr495}. Phosphatase inhibitors were shown to suppress NO production and decrease barrier function, both of which are important functions in ECs. Epigallocatechin-3-gallate (EGCG) treatment induced protein kinase A (PKA) -dependent activation of protein phosphatase-2A (PP2A) which increased MP activity. Activated MP dephosphorylated both eNOS^{pThr495} and the 20 kDa myosin II light chains at Thr18/Ser19 (ppMLC20) which resulted in relaxation of ECs. Our results suggest that the coordinated interplay between PP2A and MP accounts for the physiological regulation of eNOS activity. EGCG dependent activation of these phosphatases leads to eNOS pT495 dephosphorylation, eNOS activation, enhanced NO production and EC barrier strengthening.

Loss of EC barrier integrity results in increased vascular permeability, which often has severe consequences including the flooding of alveolar space that occurs in pneumonia. We have shown that adenosine (Ado) and ATP γ S exert their profound barrier protecting effects on HLMVEC via distinct signaling mechanisms. ATP γ S induced P2Y4 and P2Y12 mediated cAMP independent PKA activation, resulting in MP activation and ppMLC20 dephosphorylation. This pathway involves protein kinase A-anchor protein 2 (AKAP2). However, Ado-induced strengthening of the HLMVEC barrier required the coordinated activation of PKA and EPAC1 in cAMP-dependent manner.

In summary our studies shed light on the receptor-mediated phosphorylation-dephosphorylation of key endothelial proteins and identified kinases and phosphatases as well as the signaling pathways implicated in these modifications. We also show the importance of these phosphorylation-dephosphorylation events in the regulation of the physiological functions of the endothelial cells, therefore, our results may possible have pharmacological relevance.



Registry number: DEENK/296/2018.PL
Subject: PhD Publikációs Lista

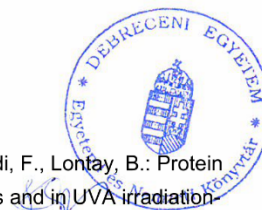
Candidate: Róbert Károly Bátor
Neptun ID: WDLNJB
Doctoral School: Doctoral School of Molecular Medicine

List of publications related to the dissertation

1. **Bátori, R. K.**, Kumar, S., Bordán, Z., Cherian-Shaw, M., Kovács-Kása, A., MacDonald, J. A., Fulton, D., Erdődi, F., Verin, A.: Differential mechanisms of adenosine- and ATPγS-induced microvascular endothelial barrier strengthening.
J. Cell. Physiol. [Epub ahead of print], 2018.
DOI: <http://dx.doi.org/10.1002/jcp.26419>
IF: 3.923 (2017)
2. **Bátori, R. K.**, Bécsi, B., Nagy, D., Kónya, Z., Hegedűs, C., Bordán, Z., Verin, A., Lontay, B., Erdődi, F.: Interplay of myosin phosphatase and protein phosphatase-2A in the regulation of endothelial nitric-oxide synthase phosphorylation and nitric oxide production.
Sci Rep. 7 (44698), 1-17, 2017.
DOI: <http://dx.doi.org/10.1038/srep44698>
IF: 4.122

List of other publications

3. Horváth, D., Sipos, A., Major, E., Kónya, Z., **Bátori, R. K.**, Dedinszki, D., Szöllősi, A. G., Tamás, I., Iván, J., Kiss, A., Erdődi, F., Lontay, B.: Myosin phosphatase accelerates cutaneous wound healing by regulating migration and differentiation of epidermal keratinocytes via Akt signaling pathway in human and murine skin.
Biochim. Biophys. Acta-Mol. Basis Dis. 1864 (10), 3268-3280, 2018.
DOI: <http://dx.doi.org/10.1016/j.bbadis.2018.07.013>
IF: 5.108 (2017)
4. Dedinszki, D., Sipos, A., Kiss, A., **Bátori, R. K.**, Kónya, Z., Virág, L., Erdődi, F., Lontay, B.: Protein phosphatase-1 is involved in the maintenance of normal homeostasis and in UVA irradiation induced pathological alterations in HaCaT cells and in mouse skin.
Biochim. Biophys. Acta-Mol. Basis Dis. 1852 (1), 22-33, 2015.
DOI: <http://dx.doi.org/10.1016/j.bbadis.2014.11.005>
IF: 5.158





5. Ruzsnavszky, O., Dienes, B., Oláh, T., Vincze, J., Gáll, T., Balogh, E., Szemán-Nagy, G., **Bátori, R. K.**, Lontay, B., Erdődi, F., Csernoch, L.: Differential Effects of Phosphatase Inhibitors on the Calcium Homeostasis and Migration of HaCaT Keratinocytes.
PLoS One. 8 (4), 1-10, 2013.
DOI: <http://dx.doi.org/10.1371/journal.pone.0061507>
IF: 3.534
6. Beyer, D., Tándor, I., Kónya, Z., **Bátori, R. K.**, Roszik, J., Vereb, G., Erdődi, F., Vasas, G., Mikóné Hamvas, M., Jambrovics, K., Máthé, C.: Microcystin-LR, a protein phosphatase inhibitor, induces alterations in mitotic chromatin and microtubule organization leading to the formation of micronuclei in *Vicia faba*.
Ann. Bot. 110 (4), 797-808, 2012.
DOI: <http://dx.doi.org/10.1093/aob/mcs154>
IF: 3.449
7. Altorjay, I., Veréb, Z., Serfőző, Z., Bacskai, I., **Bátori, R. K.**, Erdődi, F., Udvardy, M., Sipka, S., Lányi, Á., Rajnavölgyi, É., Palatka, K.: Anti-TNF-alpha antibody (infliximab) therapy supports the recovery of eNOS and VEGFR2 protein expression in endothelial cells.
Int. J. Immunopathol. Pharmacol. 24 (2), 323-335, 2011.
IF: 2.991
8. Beyer, D., Surányi, G., Vasas, G., Roszik, J., Erdődi, F., Mikóné Hamvas, M., Bácsi, I., **Bátori, R. K.**, Serfőző, Z., Máthéné Szigeti, Z., Vereb, G., Demeter, Z., Gonda, S., Máthé, C.: Cylindrospermopsin induces alterations of root histology and microtubule organization in common reed (*Phragmites australis*) plantlets cultured in vitro.
Toxicol. 54 (4), 440-449, 2009.
DOI: <http://dx.doi.org/10.1016/J.toxicol.2009.05.008>
IF: 2.128
9. Palatka, K., Serfőző, Z., Veréb, Z., **Bátori, R. K.**, Lontay, B., Hargitay, Z., Nemes, Z., Udvardy, M., Erdődi, F., Altorjay, I.: Effect of IBD sera on expression of inducible and endothelial nitric oxide synthase in human umbilical vein endothelial cells.
World J. Gastroenterol. 12 (11), 1730-1738, 2006.
DOI: <http://dx.doi.org/10.3748/wjg.v12.i11.1730>.

Total IF of journals (all publications): 30,413

Total IF of journals (publications related to the dissertation): 8,045

The Candidate's publication data submitted to the iDEa Tudóstér have been validated by DEENK on the basis of Web of Science, Scopus and Journal Citation Report (Impact Factor) databases.

06 September, 2018

